JOURNAL OF MAGNETIC RESONANCE **124,** 468–473 (1997)
ARTICLE NO. MN961082

Determination of Oligomeric State of Proteins in Solution from Pulsed-Field-Gradient Self-Diffusion Coefficient Measurements. A Comparison of Experimental, Theoretical, and Hard-Sphere Approximated Values

V. V. KRISHNAN*

Department of Structural Biology, The Burnham Institute,† 10901 North Torrey Pines Road, La Jolla, California 92037

Received November 22, 1996

The first step toward protein structure determination using NMR is elucidation of the appropriate solution conditions that obviate any protein self-association at the millimolar concentration necessary for the analysis (*1*). Knowledge on the oligomerization of the protein prior to the data collection is rather important, due to the complexity associated with assigning and identifying long-range nuclear Overhauser effect (NOE) contacts in the process of determining the three-dimensional structure (*2*). In general, the oligomerization state of a protein of interest is characterized using biophysical methods like equilibrium ultracentrifugation or dynamic light scattering measurements (*3*). Even though reliable results are obtained in most cases, these measurements are done at a much lower protein concentration, which differs about three orders of magnitude compared to the sample concentration for the NMR experiments. Hence, determination of the oligomerization state of the protein under the sample conditions of the NMR experiments is primarily important.

The use of pulsed magnetic field gradients in high-resolution NMR is a major advancement due to the availability of self-shielded gradient coils in commercial spectrometers (*4, 5*). Among the many potential applications of pulsed field gradients (PFG) are the reduction in the number of phase-cycling steps needed for a specific coherence-transfer pathway and efficient cancellation of spectral artifacts (*6, 7*). In addition to the modern applications of PFG in biomolecular NMR (*6, 7*), classical experimental methods to measure self-diffusion coefficients using PFG (*8*) have been applied to proteins and DNA oligomers to understand the molecular association processes (*9–18*).

PFG NMR has been widely used to measure tracer diffusion coefficients of small molecules and polymers in solution (*16*). However, only a few reports describe the measurement of self-diffusion coefficient in peptides (*17, 18*), proteins (*9–14*), and DNA oligomers (*15*). Altieri *et al.* (*12*) have recently adopted the LED (*l*ongitudinal *e*ncode–*d*ecode) experiment proposed by Gibbs and Johnson (*19*), with an improved water suppression scheme, to measure self-diffusion coefficients of proteins. Ratio of the experimentally measured diffusion constants was used in comparison with the expected ratio for a hard-sphere contact of monomers to determine the oligomerization state of proteins (*9, 12*). This method provides a quick way to measure the oligomerization state of proteins under the NMR sample conditions.

The purpose of the present note is to evaluate how well the hard-sphere approximation of dimer formation is adapted in determining the oligomerization state of proteins. This is achieved by measuring the self-diffusion coefficient experimentally, using the LED sequence, as well as calculating it theoretically using the beads theory of García de la Torre (*20*) on a set of proteins of known oligomerization state. When these results are compared with the ratios obtained by approximating the formation of dimers as hard-sphere monomer contacts, only a qualitative agreement is obtained. Experimentally measured self-diffusion coefficients show a larger dispersion with the ideal molecular weights obtained from amino-acid composition, compared to the calculated values. The origin of such a difference is ascribed to the interaction of the protein with the solvent medium. It has also been found that self-diffusion coefficients obtained experimentally as well theoretically correlate linearly with the solvent-accessible surface area (*21, 22*), providing an additional parameter to represent quaternary structure of proteins.

The basis of the LED-PFG sequence is the use of bipolar gradient pulses (*19, 23, 24*) to minimize eddy-current effects. As in the conventional stimulated-echo experiment of Tanner (*25*), a pair of matched gradient pulses are separated by the interval $(\Delta - \delta)$, each having an effective area of q, where q is a product of $\gamma g_z \delta$, with γ the gyromagnetic ratio of protons, and g_z and δ the amplitude and duration of the z gradient

* Currrent address: Biology and Biotechnology Research Program, Lawrence Livermore National Laboratory, L-452, Livermore, CA 94551.
† Formerly La Jolla Cancer Research Foundation.

1090-7807/97 $25.00

pulse (*19*). Information on translational diffusion is encoded by varying q, and generally g_z is varied between experiments. The signal is detected as a free-induction decay, and Fourier transform with respect to time yields a spectrum with the peak intensities given by the relation (*26*)

$$f(q) = \int dD R(T_1, T_2) G(D_S) \times \exp\left[-D_S q^2 \left(\Delta - \frac{\delta}{3} \right) \right], \quad [1]$$

where $R(T_1, T_2)$ is the attenuation due to relaxation processes and $G(D_S)$ is the mass-weighted distribution of self-diffusion coefficient (D_S). For monodisperse samples, $G(D_S)$ is a delta function and the slope of the plot between $\ln[f(q)]$ versus $q^2(\Delta - \delta/3)$ yields the self-diffusion coefficient. For polydisperse samples, typically a mixture of polymers in solution, a much more detailed analysis of the data is necessary (*26, 27*). Under the conditions of negligible relaxation and molecular weight dispersion, the product $R(T_1, T_2)G(D_S)$ in Eq. [1] can be replaced by unity (*26, 27*).

In the present case, the self-diffusion coefficient (D_S^{expt}) was measured experimentally for six proteins; C-terminal domain of the α subunit of the RNA polymerase (αCTD), calbindin-D_{9k}, calcyclin, PU.1, lysozyme, and transcription factor-1 (TF1) using the water-LED sequence (*12*). In addition, D_S values reported using the same method for interleukin-10, monocyte chemotactic protein-1 (MCP-1), and ubiquitin were also considered as part of the experimental set of D_S. It may be mentioned that D_S values for lysozyme presented in this case agree well with the reported value (*12*). In the collection of proteins considered here, calcyclin, TF1, interleukin-10, and MCP-1 are established as dimers and the rest are monomers under NMR sample conditions. Concentration of all the protein samples were between 1 and 2 mM in water (90% H_2O, 10% ^2H_2O) with the exception of TF1 (100% ^2H_2O). No correction on D_S for the change of solvent viscosity from H_2O to ^2H_2O was applied (*11*). A total volume of 450 μl was used for calbindin-D_{9k} and calcyclin, while 600 μl was used for the others in standard NMR sample tubes (Wilmad Inc., 528 pp).

Self-diffusion coefficients were measured using the pulse sequence by Altieri *et al.* (*12*) in a Varian Unity*plus* (ν_H = 500 MHz) NMR spectrometer, equipped with a triple-resonance pulsed-field-gradient probe with an actively shielded *z*-gradient coil and a gradient amplifier to generate a maximum gradient strength of 32 G cm^{-1}. The gradient strength (g_z) was calibrated with reference to the self-diffusion coefficient of residual H_2O in doped ^2H_2O (0.1 mg/ml of $GdCl_3$) (*28*). Pulse widths were optimized for each protein and g_z was varied from 5 to 32 G cm^{-1}, in steps of 1 G cm^{-1}. The acquisition time for each transient was 0.655 s over a spectral width of 12,500 Hz, and each FID was signal averaged over 32 transients with a recycling delay of 4 s. Time-domain data was zero filled once and Fourier transformed with no apodization. The area under each spectrum from 3.5 to −0.5 ppm was integrated, and a nonlinear least-squares fit (*29*) was used to estimate D_S^{expt}. Triplicate experimental measurements were performed only on proteins αCTD and TF1. Table 1 lists the experimentally determined self-diffusion constants (D_S^{expt}) of all the proteins (*30*).

Translational self-diffusion coefficients (D_S^{calc}) are calculated based on the beads model approximation of García de la Torre (*20*). This method has been used successfully by several groups to calculate the translational and rotational diffusion coefficients of proteins as well as nucleic acids (*31–33*). The program DIFFC based on the beads theory and developed by Arseniev and co-workers (*33*) has been used for the present calculation. In this method, the protein is modeled as a collection of point sources of friction (denoted as beads) with hydrodynamic Ossen tensor interactions between them (*20*). A set of linear equations are then obtained for the N specified atoms from the three-dimensional structure of the protein, and the solution of the array is obtained by numerically inverting a $3N \times 3N$ matrix to calculate the translational frictional tensor and hence the self-diffusion coefficient, D_S^{calc}.

For all the nine proteins considered here, three-dimensional structures of the protein itself or a protein of the same family determined either by NMR or by X-ray crystallography are available (*34–44*). The coordinates of NMR determined structures for αCTD (*34*), calbindin-D_{9k} (*35*), and lysozyme (*36*) and crystal structure coordinates of interleukin-10 (*37*) and ubiquitin (*38*) were obtained from the protein data bank (Brookhaven National Laboratory). The coordinates for calcyclin (*39*) and TF1 (*40*) were kindly provided by Dr. B. C. M. Potts and Dr. X. Jia (personal communication), respectively. For proteins MCP-1 (*41*) and PU.1 (*42*), equivalent NMR-determined structures of RANTES (*43*) and ETS-1 (*44*) are considered. All the backbone atoms are considered as beads of equal size (σ = 5.0 Å) (*20, 33*) at a temperature of 303 K in water (viscosity η = 0.7982 Ns m^{-2}). Table 1 also lists D_S^{calc} obtained as the trace of the diffusion tensor. Theoretically calculated self-diffusion constants are higher than the experimental values, as this procedure of calculation assumes an infinite dilution of protein in the absence of intermolecular interactions (*32*).

In order to derive useful information on the oligomerization state, it was proposed by several groups that a ratio of the self-diffusion coefficients can be utilized as a signature of the molecular association process by approximating the monomer–monomer contact as hard-sphere molecular contact (*9, 12, 20, 45*). Using the hydrodynamic calculations, the ratio of the diffusion constants of a n-mer [$D_S(n)$] to that of a monomer [$D_S(m)$] can be given by (*20, 45*)

$$R = \frac{D_S(n)}{D_S(m)} = F_n n^{-1/3}, \quad [2]$$

TABLE 1
Self-Diffusion Coefficient of Proteins and Associated Parameters

Oligomer[a]	Proteins	Code	D_S^{expt},[b] ($\times 10^{-9}$ m^2 s^{-1})	D_S^{calc},[d] ($\times 10^{-9}$ m^2 s^{-1})	Molecular weight (kD)	SASA[e] (Å^2)	Reference[f]
Monomer	Calbindin-D_{9k}	CB	11.09[g]	17.28	8.4	4,651	*35*
	Ubiquitin	UB	14.90[c]	16.47	8.6	4,768	*12, 38*
	α subunit of RNA polymerase	AS	9.10[g]	15.75	9.6	5,888	*34*
	PU-1	PU	10.66[g]	14.80	12.6	7,325	*42, 44*
	Lysozyme	LY	10.86[c,g]	14.06	14.1	7,384	*36*
Dimer	Monocyte chemotactic protein-1	MC	10.80[c]	12.62	17.4	9,379	*41, 43*
	Calcyclin	CC	7.15[g]	12.39	20.1	9,833	*39*
	Transcription factor 1	TF	6.36[g]	11.34	21.4	12,009	*40*
	Interleukin-10	IL	8.20[c]	11.28	17.2	12,235	*12, 37*

[a] Molecules are monomers or dimers under the NMR sample conditions as given in the corresponding references describing the three-dimensional structures.

[b] Estimated error in the experimental measurements of self-diffusion constants is $\pm 0.04 \times 10^{-9}$ m^2 s^{-1}. Errors are estimated from the triplicate measurements only in the proteins αCTD and TF-1.

[c] From the published results of Ref. (*12*).

[d] Calculated using the program DIFFC (*33*), for all backbone atoms with a scaling factor of 5 Å at 303 K in water.

[e] SASA: Solvent-accessible surface area, calculated using QUANTA (Molecular Simulations Inc.) with a probe radius of 1.4 Å and a surface point density of 20 on a silicon graphics workstation.

[f] Co-ordinates of NMR-determined structures were used, whenever available (Protein data bank, Brookhaven National Laboratories). Structures for MCP-1 (*41*) and PU.1 (*42*) have been substituted with that of RANTES (*43*) and ETS-1 (*44*) respectively. X-ray crystallography-determined structures have been used for interleukin-10 and ubiquitin.

[g] Presented in part in Ref. (*30*).

where F_n is a geometric factor. Equation [2] has been derived independently by Teller *et al.* (*45*) and García de la Torre *et al.* (*20*), and their ratios for the formation of dimers ($n = 2$) were 0.749 [Table I of Ref. (*45*)] and 0.725 [Table III of Ref. (*20*)], respectively. These references provide ratios in the case of linear trimer as 0.598 and 0.586 and for equilateral trimers as 0.662 and 0.621. A third value of 0.719 was obtained by Wills *et al.* (*9*) under the same approximation, a value close to the ratio obtained by García de la Torre *et al.* (*20*). Even for a simple approximation of hard-sphere monomer–monomer contact, the estimated ratio of diffusion coefficients varies depending on the choice of the method used for calculation (*20*). In view of the differences in hard-sphere approximated ratio of self-diffusion coefficients for dimer formation (*9, 20, 45*), an average of all the above three values, 0.731, can be considered.

Figure 1 shows the plot of the experimentally obtained ratio of self-diffusion coefficients [D_S^{expt}(d)/D_S^{expt}(m), d for dimer] versus the corresponding values calculated theoretically [D_S^{calc}(d)/D_S^{calc}(m)]. The average hard-sphere approximated value (0.731) is also marked in Fig. 1 by a dotted line. The proteins are identified by the two-letter code given in Table 1 as well in the legend to Fig. 1. The protein pairs falling in the range of 0.70 to 0.80 in both axes of Fig. 1 show a good correlation as a dimer–monomer pair. Protein pairs (IL, PU) and (CC, AS) have molecular weight ratios close to 2.0, and for these pairs, both experimental and theoretical diffusion constants ratios also agree well.

None of the protein pairs investigated here, however, give the hard-sphere approximation value from the ratios obtained from theory and experiment simultaneously. The protein pair (IL, CB) gives an experimental ratio of 0.74, close to the hard-sphere value, but the theoretical ratio of 0.65 is a hard-sphere approximated value close to that of an equilateral trimer. On the other hand, the protein pair (CC, UB) shows an trend opposite to that of the protein pair (IL, CB) in which the theoretical ratio is close to the hard-sphere dimer approximation. In using the method of ratios to determine protein dimers or monomers in solution, it is important to choose a reference protein that is respectively half or twice the molecular weight to form the corresponding dimer–monomer pair. For example, the calculated and experimental ratios of the protein pairs (IL, UB), (CC, UB), and (TF, UB) are very much different from the hard-sphere approximated value, as the molecular weight of ubiquitin is not close to half the molecular weights of interleukin-10, calcyclin, and TF1. Figure 1 also shows a larger dispersion in the ratios of D_S^{expt} compared to the calculated ratios. As it may be practically difficult to find identical conditions for all the proteins, the dispersion in D_S^{expt} has been ascribed to the wider distribution under the sample conditions.

These results suggest that, although the hard-sphere approximation is a fast and easy way to estimate the oligomerization state (in this case dimers) of proteins, the results are qualitative and must be interpreted with care. It further emphasizes that the ratio must be compared with at least

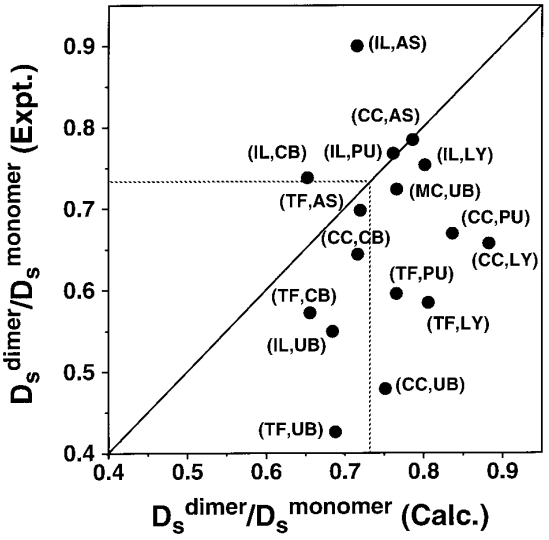

FIG. 1. Plot of the experimentally obtained ratio of the self-diffusion coefficient of a dimer to a monomer and the corresponding ratios calculated using the hydrodynamic theory. Each point in the graph is the ratio of diffusion coefficient for a dimer–monomer pair, and the proteins are identified by two-letter codes; α subunit of the RNA polymerase (AS), calbindin-D_{9k} (CB), PU.1 (PU), lysozyme (LY), ubiquitin (UB), calcyclin (CC), interleukin-10 (IL), monocyte chemotactic protein-1 (MC), and transcription factor-1 (TF). The average value of the ratios of the dimer–monomer diffusion constant (0.731) under the approximation of hard-sphere monomer–monomer contacts calculated by Teller *et al.* (*45*) (0.749), García de la Torre *et al.* (*20*) (0.725), and Wills *et al.* (*9*) (0.719) is given by the dashed line.

several reference proteins of previously known oligomerization states to avoid any possible pitfalls. For example, in the case of αCTD, the ratios with both calcyclin and TF-1 suggest it to be a monomer (*30*), and in the case of interleukin-10 the ratios with lysozyme and PU.1 confirm it to be a dimer.

In calculating the self-diffusion coefficients, the beads can be modeled as exact representation of the respective atoms of the protein (*20, 32, 33*), instead of atoms of equal radii. The former approach, although computationally demanding, allows a detailed description of the irregular surfaces of the molecules (*32, 33*). It has been noticed that considering all the atoms, although it decreases the calculated diffusion constant, does not alter the ratios between them. Hence, in the present case, assuming the error in D_S^{calc} is approximately the same for all proteins, the ratio of the diffusion constants is prone to the least error.

Self-diffusion coefficients can also be used quantitatively to determine molecular weights of proteins following the relation (*46*),

$$M_w = \left(\frac{k_B T}{6\pi\eta F D_S}\right)^3 \left(\frac{4\pi N_0}{3(\bar{V}_2 + \delta_1 \bar{V}_1)}\right), \qquad [3]$$

where k_B is the Boltzmann constant (1.3806×10^{-23} m^{2}kg s^{-2} K^{-1}); T is temperature in K; η is viscosity of the solvent; N_0 is Avogadro's number (6.02217×10^{23} mol^{-1}), $\bar{V}_1$ and $\bar{V}_2$ are partial specific volumes of the protein and the solvent molecule (in m^{3}kg^{-1}); δ_1 is the fractional amount of water bound to the protein (grams of water per gram of protein); and F is Perkin's shape factor (*46*). Once the partial specific volume of the protein is calculated from the amino acid composition following the recipe of Perkins (*47*), at a given temperature, the molecular weight of the protein is inversely related to D_S through the parameters F and δ_1 (Eq. [3]). If additional experimental information can be obtained on F and δ_1 as in the study of association of myosin light chain 2 (MLC2) molecules with the zwitterionic bile salt derivative (CHAPS), quantitative information on the molecular association process can be obtained in a reliable manner (*14*). In general, F and δ_1 are not known a priori without the knowledge of the three-dimensional structure of the protein. If δ_1 in Eq. [3] is used as a variable parameter and for a sphere ($F = 1$), most of the experimental self-diffusion coefficients (D_S^{expt}) listed in Table 1 need at least three hydration shells (for 0.328 *g* of water per gram of protein) to match the ideal molecular weights (data not shown).

It has been known from the literature that hydration shells must be considered explicitly to obtain a reasonable agreement between the experimental and theoretical values of the self-diffusion coefficient (*32, 48*). An alternate approach is to use a molecular dynamics simulation in water to obtain a close match (*49*). García de la Torre and Bloomfield (*20*) have shown that, although hydration complicates the quantitative analysis, it does not interfere with the determination of the hydrodynamic properties if one assumes that monomer hydration remains constant upon oligomerization. The self-diffusion coefficients of proteins can also be used efficiently in the equations of Wang (*50*) to determine the density of water molecules surrounding the protein (*51, 52*).

A parameter that relates closely to the protein surface and the solvent is the ''solvent-accessible surface area'' (*21, 22*), and it is one of the important structural parameters that determines the stability of the protein folding, complexation, and quaternary structural rearrangements (*53, 54*). According to the algorithm of Lee and Richards (*21*), the solvent-accessible surface area is defined as the area swept out by the center of a sphere resembling a water molecule while the sphere rolls over the van der Waals surface of the protein. The solvent-accessible surface area of all the nine proteins has been calculated using Quanta (Molecular Simulations Inc.) with a probe radius of 1.4 Å and surface-point density of 20 for all the protein atoms. Table 1 also lists the solvent-accessible surface area for all the proteins. Figure 2 shows the plot of the correlation between the solvent-accessible surface area and the self-diffusion coefficients obtained from theory (Fig. 2a) and experiments (Fig. 2b). D_S^{calc} and D_S^{expt} give a linear correlation coefficients (*55*) of $-0.98 \pm$

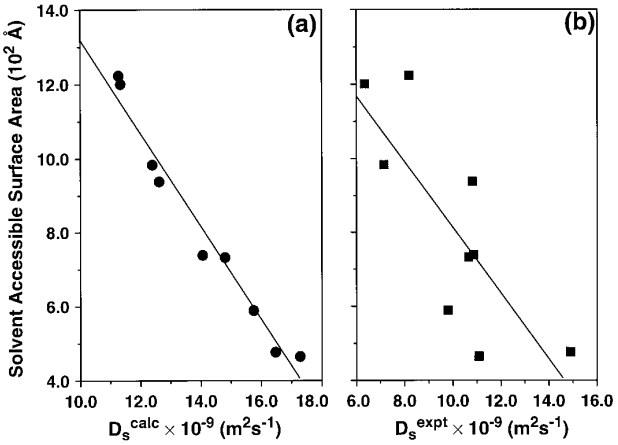

FIG. 2. Self-diffusion coefficients obtained experimentally using the PFG-LED (*12*) sequence and calculated by the hydrodynamic beads theory of García de la Torre *et al.* (*20, 33*) are plotted against the solvent-accessible surface area of the proteins calculated in (a) and (b), respectively. Solvent-accessible surface area was calculated with a probe radius of 1.4 Å and a surface-point density of 20 using QUANTA (Molecular Simulations Inc.) from the three-dimensional structure. The size of the symbols in the plot of the experimental values of the self-diffusion coefficient is approximately equal to the error in the measurement. The theoretical and experimental values correlated linearly with the solvent-accessible surface area with correlation coefficients (*55*) of -0.98 ± 0.08 and -0.79 ± 0.26, respectively.

0.08 and -0.79 ± 0.26 respectively with a larger dispersion in the experimental values. This empirical correlation provides an additional structural parameter relating the self-diffusion coefficient and solvent-accessible surface area.

It may be mentioned that Venable and Pastor (*32*) have used a similar parameter, called accessible surface area (ASA), to determine the hydration parameters of proteins and peptides from the theoretically calculated translational diffusion coefficients. The ASA for proteins is calculated by constructing a grid of cubes 1.6 Å on a side around the protein and filling those cells adjacent to, but not occupied by the protein (*32*). It can be expected that ASA would also show a correlation similar to that of SASA. As the self-diffusion constant measurements on more proteins become available, the current empirical correlation between the self-diffusion coefficient and solvent-accessible surface area is expected to refine to a statistically significant value.

In conclusion, self-diffusion coefficient measurements in the presence of pulsed magnetic field gradients and the use of dimer-to-monomer ratio of these coefficients provide an efficient method for determining the oligomeric state of proteins to screen for the optimal sample conditions under which NMR experiments are performed. The self-diffusion coefficient was measured using the LED sequence and calculated using the hydrodynamic theory for a set of nine proteins of known state of oligomerization (monomer or dimer). Experimental and theoretical ratios of diffusion constants of dimer-to-monomer agree qualitatively with the corresponding ratios obtained from hard-sphere approximation of monomer–monomer contact. Experimental values of the self-diffusion coefficient are sensitive to the inherent properties of the protein in solution (for example, hydration), and hence, the ratio of diffusion constants can vary significantly depending on the sample conditions. Hence, it may be necessary to compare the results with more than one reference protein in order to avoid possible pitfalls of the methodology. In addition, it has been noted that solvent-accessible surface areas of the proteins correlate linearly, providing with NMR-determined self-diffusion coefficient as an additional parameter to describe quaternary structures.

ACKNOWLEDGMENTS

The author thanks Drs. N. Murali and L. Renuka for critical reading of the manuscript. Thanks also go to Professor Arseniev and co-workers at the Russian Academy of Sciences for the program DIFFC. Drs. N. Assa-Munt, W. J. Chazin, and X. Jia are acknowledged for the loan of the proteins samples, αCTD and PU.1, Calbindin-D_{9k} and Calcyclin, and TF1, respectively. The NMR spectrometer was purchased from a grant to the Burnham Institute (formerly La Jolla Cancer Research Foundation) by the Lucille P. Markey Foundation.

REFERENCES

1. N. J. Oppenheimer, *in* ''Nuclear Magnetic Resonance, Part A'' (N. J. Oppenheimer and T. L. James, Eds.), Methods in Enzymology, Vol. 176, pp. 78–89, Academic Press, San Diego, 1989.
2. (*i*) K. Wüthrich, ''NMR of Proteins and Nucleic Acids,'' Wiley, New York, 1986; (*ii*) G. M. Clore and A. M. Gronenborn, *Protein Sci.* **3,** 372–390 (1994).
3. K. E. van Holde, ''Physical Chemistry,'' 2nd ed., Prentice–Hall, Englewood Cliffs, New Jersey, 1985.
4. P. Mansfield and B. Chapman, *J. Magn. Reson.* **66,** 573–576 (1986).
5. R. E. Hurd, *J. Magn. Reson.* **87,** 422–428 (1990).
6. J. Keller, R. T. Clowes, A. L. Davis, and E. D. Laue, *in* ''Nuclear Magnetic Resonance, Part C'' (T. L. James and N. J. Oppenheimer, Eds.), Methods in Enzymology, Vol. 239, pp. 145–207, Academic Press, San Diego, 1994.
7. L. E. Kay, *Curr. Opin. Struct. Biol.* **5,** 674–681 (1995).
8. E. O. Stejskal and J. E. Tanner, *J. Chem. Phys.* **42,** 288–292 (1965).
9. P. R. Wills and Y. Geogalis, *J. Phys. Chem.* **85,** 3978–3984 (1981).
10. C. H. Everhart and C. S. Johnson Jr., *Biopolymers* **21,** 2049–2054 (1982).
11. R. L. Haner and T. Schleich, *in* ''Nuclear Magnetic Resonance, Part A'' (N. J. Oppenheimer and T. L. James, Eds.), Methods in Enzymology, Vol. 176, pp. 418–446, Academic Press, San Diego, 1989.
12. A. M. Altieri, D. P. Hilton and R. A. Byrd, *J. Am. Chem. Soc.* **117,** 7566–7567 (1995).
13. M. Lin and C. K. Larive, *Anal. Biochem.* **229,** 214–220 (1995).
14. A. J. Dingley, J. P. Mackay, B. E. Chapman, M. B. Morris, P. W. Kuchel, B. D. Hamply, and G. F. King, *J. Biomol. NMR* **6,** 321–328 (1995).

15. B. Andreasson, L. Nordenskiöld, W. H. Braunlin, J. Schultz, and P. Stlibs, *Biochemistry* **32,** 961–967 (1993).
16. P. Stlibs, *Prog. NMR Spectrosc.* **19,** 1–45 (1987).
17. V. A. Daragan, E. Ilyina, and K. H. Mayo, *Biopolymers* **33,** 521–533 (1993).
18. K. H. Mayo, E. Ilyna, and H. Park, *Protein Sci.* **5,** 1301–1315 (1996).
19. S. J. Gibbs and C. S. Johnson Jr., *J. Magn. Reson.* **93,** 395–402 (1991).
20. J. García de la Torre and N. A. Bloomfield, *Q. Rev. Biophys.* **14,** 81–139 (1981).
21. B. Lee and F. M. Richards, *J. Mol. Biol.* **55,** 379–400 (1971).
22. T. J. Richmond and F. M. Richards, *J. Mol. Biol.* **119,** 537–555 (1978).
23. R. M. Boerner and W. S. Woodward, *J. Magn. Reson. A* **106,** 195–202 (1994).
24. D. Wu, A. Chen, and C. S. Johnson Jr., *J. Magn. Reson. A* **115,** 260–264 (1995).
25. J. E. Tanner, *J. Chem. Phys.* **52,** 2523–2526 (1970).
26. A. Chen, D. Wu, and C. S. Johnson Jr., *J. Am. Chem. Soc.* **117,** 7965–7970 (1995).
27. P. Stilbs, K. Paulsen, and P. C. Griffiths, *J. Phys. Chem.* **100,** 8180–8189 (1996).
28. L. G. Longsworth, *J. Phys. Chem.* **64,** 1914–1917 (1960).
29. W. H. Press, B. P. Flannery, S. A. Teukolsky, and W. T. Vetterling, ''Numerical Recipes: The Art of Scientific Computing,'' p. 521, Cambridge Univ. Press, New York, 1988.
30. X. Jia, V. V. Krishnan, E. Blatter, R. H. Ebright, and N. Assa-Munt, Abstracts of the 37th Experimental NMR Conference, Abstract MP-48, March 17–22, 1996.
31. W. Eimer, J. R. Williamson, S. G. Boxer, and R. Pecora, *Biochemistry* **29,** 799–811 (1990).
32. R. M. Venable and R. W. Pastor, *Biopolymers* **27,** 1001–1014 (1988).
33. V. Yu-Orekhov, D. E. Nolde, A. P. Golovanov, D. M. Dorzhnev, and A. S. Arseniev, *Appl. Magn. Reson.* **9,** 581–588 (1995).
34. Y. H. Jeon, T. Negishi, M. Shirakawa, T. Yamazaki, N. Fujita, A. Ishihama, and Y. Kyogoku, *Science* **270,** 1495–1497 (1995).
35. N. J. Skelton, J. Kördel, and W. J. Chazin, *J. Mol. Biol.* **249,** 441–462 (1993).
36. L. J. Smith, M. J. Sutcliffe, C. Redfield, and C. M. Dobson, *J. Mol. Biol.* **229,** 930–944 (1993).
37. A. Zdanov, C. Schal-hihi, A. Gustchina, M. Tsang, J. Weatherbee, and A. Wlodawer, *Structure* **3,** 591–601 (1995).
38. S. Vjaykumar, C. E. Bugg, and W. J. Cook, *J. Mol. Biol.* **194,** 531–544 (1987).
39. B. C. M. Potts, J. Smith, M. Akke, T. J. Macke, K. Okazaki, H. Hidaka, D. A. Case, and W. J. Chazin, *Nat. Struct. Biol.* **2,** 790–796 (1995). Addition/Correction; *Nat. Struct. Biol.* **2,** 912 (1995).
40. X. Jia, A. Grove, M. Ivancic, V. L. Hsu, E. P. Geiduschek, and D. R. Kearns, *J. Mol. Biol.* **263,** 259–268 (1996).
41. T. M. Handel and P. J. Domaille, *Biochemistry* **35,** 6569–6584 (1996).
42. R. Kodandapani, F. Pio, C. Z. Ni, G. Piccialli, M. Klemsz, S. McKercher, R. A. Maki, and K. R. Ely, *Nature* **380,** 456–460 (1996).
43. N. J. Skelton, F. Aspiras, J. Ogez, and T. J. Schall, *Biochemistry* **34,** 5329–5342 (1995).
44. L. W. Donaldson, J. M. Petersen, B. J. Graves, and L. P. McIntash, *EMBO J.* **15,** 125–134 (1996).
45. D. C. Teller, E. Swanson, and C. de Haën, *in* ''Enzyme Structure, Part H'' (C. H. W. Hirs and S. N. Timasheff, Eds.), Methods in Enzymology, Vol. 61, pp. 103–124, 1979.
46. C. R. Cantor and P. R. Schimmel, ''Biophysical Chemistry, Part II, Techniques for the Study of Biological Structure and Function,'' Chap. 10, W. H. Freeman, San Francisco, 1980.
47. S. J. Perkins, *Eur. J. Biochem.* **157,** 169–180 (1986).
48. P. G. Squire and M. E. Himmel, *Arch. Biochem. Biophys.* **196,** 165–167 (1979).
49. P. E. Smith and W. F. van Gunstern, *J. Mol. Biol.* **236,** 629–635 (1994).
50. J. H. Wang, *J. Am. Chem. Soc.* **76,** 4755–4763 (1954); J. H. Wang, C. B. Anfinsen and F. M. Polestra, *J. Am. Chem. Soc.* **76,** 4763–4765 (1954).
51. D. Bourret and J. Parello, *J. Phys.* **C7,** 255–258 (1984).
52. H. M. Baranowska and K. J. Olszewski, *Biochem. Biophys. Acta* **1289,** 312–314 (1996).
53. D. Eisenberg and A. D. McLachlan, *Nature* **319,** 199–203 (1986).
54. T. J. Richmond, *J. Mol. Biol.* **178,** 2133–2141 (1984).
55. W. H. Press, B. P. Flannery, S. A. Teukolsky, and W. T. Vetterling, ''Numerical Recipes: The Art of Scientific Computing,'' p. 484, Cambridge Univ. Press, New York, 1988.